Raman amplification of pure side-seeded higher-order modes in hydrogen-filled hollow-core PCF

Jean-Michel Ménard,[*] Barbara M. Trabold, Amir Abdolvand, and Philip St.J. Russell

Max Planck Institute for the Science of Light, Günther-Scharowsky-Straße 1, 91058 Erlangen, Germany
[*]jean-michel.menard@mpl.mpg.de

Abstract: We use Raman amplification in hydrogen-filled hollow-core kagomé photonic crystal fiber to generate high energy pulses in pure single higher-order modes. The desired higher-order mode at the Stokes frequency is precisely seeded by injecting a pulse of light from the side, using a prism to select the required modal propagation constant. An intense pump pulse in the fundamental mode transfers its energy to the Stokes seed pulse with measured gains exceeding 60 dB and output pulse energies as high as 8 µJ. A pressure gradient is used to suppress stimulated Raman scattering into the fundamental mode at the Stokes frequency. The growth of the Stokes pulse energy is experimentally and theoretically investigated for six different higher-order modes. The technique has significant advantages over the use of spatial light modulators to synthesize higher-order mode patterns, since it is very difficult to perfectly match the actual eigenmode of the fiber core, especially for higher-order modes with complex multi-lobed transverse field profiles.

OCIS codes: (060.5295) Photonic crystal fibers; (190.5890) Scattering, stimulated.

References and links

1. R. Cherif, M. Zghal, L. Tartara, and V. Degiorgio, "Supercontinuum generation by higher-order mode excitation in a photonic crystal fiber," Opt. Express **16**(3), 2147–2152 (2008).
2. N. Bozinovic, Y. Yue, Y. Ren, M. Tur, P. Kristensen, H. Huang, A. E. Willner, and S. Ramachandran, "Terabit-Scale Orbital Angular Momentum Mode Division Multiplexing In Fibers," Science **340**(6140), 1545–1548 (2013).
3. O. A. Schmidt, T. G. Euser, and P. St. J. Russell, "Mode-based microparticle conveyor belt in air-filled hollow-core photonic crystal fiber," Opt. Express **21**(24), 29383–29391 (2013).
4. J. A. Pechkis and F. K. Fatemi, "Cold atom guidance in a capillary using blue-detuned, hollow optical modes," Opt. Express **20**(12), 13409–13418 (2012).
5. W. Löffler, T. G. Euser, E. R. Eliel, M. Scharrer, P. St. J. Russell, and J. P. Woerdman, "Fiber Transport of Spatially Entangled Photons," Phys. Rev. Lett. **106**(24), 240505 (2011).
6. C. Gabriel, A. Aiello, W. Zhong, T. G. Euser, N. Y. Joly, P. Banzer, M. Förtsch, D. Elser, U. L. Andersen, Ch. Marquardt, P. St. J. Russell, and G. Leuchs, "Entangling Different Degrees of Freedom by Quadrature Squeezing Cylindrically Polarized Modes," Phys. Rev. Lett. **106**(6), 060502 (2011).
7. L. Carbone, C. Bogan, P. Fulda, A. Freise, and B. Willke, "Generation of High-Purity Higher-Order Laguerre-Gauss Beams at High Laser Power," Phys. Rev. Lett. **110**(25), 251101 (2013).
8. T. G. Euser, G. Whyte, M. Scharrer, J. S. Y. Chen, A. Abdolvand, J. Nold, C. F. Kaminski, and P. St. J. Russell, "Dynamic control of higher-order modes in hollow-core photonic crystal fibers," Opt. Express **16**(22), 17972–17981 (2008).
9. R. Ismaeel, T. Lee, B. Oduro, Y. Jung, and G. Brambilla, "All-fiber fused directional coupler for highly efficient spatial mode conversion," Opt. Express **22**(10), 11610–11619 (2014).
10. J. E. Midwinter, "The prism-taper coupler for the excitation of single modes in optical transmission fibres," Opt. Quantum Electron. **7**(4), 297–303 (1975).
11. D.-I. Yeom, H. C. Park, I. K. Hwang, and B. Y. Kim, "Tunable gratings in a hollow-core photonic bandgap fiber based on acousto-optic interaction," Opt. Express **17**(12), 9933–9939 (2009).
12. V. R. Daria, P. John Rodrigo, and J. Glückstad, "Programmable complex field coupling to high-order guided modes of micro-structured fibres," Opt. Commun. **232**(1–6), 229–237 (2004).
13. N. Bozinovic, S. Golowich, P. Kristensen, and S. Ramachandran, "Control of orbital angular momentum of light with optical fibers," Opt. Lett. **37**(13), 2451–2453 (2012).

14. J. W. Nicholson, J. M. Fini, A. M. DeSantolo, E. Monberg, F. DiMarcello, J. Fleming, C. Headley, D. J. DiGiovanni, S. Ghalmi, and S. Ramachandran, "A higher-order-mode erbium-doped-fiber amplifier," Opt. Express **18**(17), 17651–17657 (2010).
15. S. Ramachandran, J. M. Fini, M. Mermelstein, J. W. Nicholson, S. Ghalmi, and M. F. Yan, "Ultra-large effective-area, higher-order mode fibers: a new strategy for high-power lasers," Laser Photon. Rev. **2**(6), 429–448 (2008).
16. B. M. Trabold, D. Novoa, A. Abdolvand, and P. St. J. Russell, "Selective excitation of higher order modes in hollow-core PCF via prism-coupling," Opt. Lett. **39**(13), 3736–3739 (2014).
17. B. M. Trabold, A. Abdolvand, T. G. Euser, A. M. Walser, and P. St. J. Russell, "Amplification of higher-order modes by stimulated Raman scattering in H2-filled hollow-core photonic crystal fiber," Opt. Lett. **38**(5), 600–602 (2013).
18. J. F. Reintjes, "Stimulated Raman and Brillouin Scattering," in *Handbook of Laser Science and Technology, Supplement 2: Optical Materials,* W. M. J., ed. (CRC, 1995), p. 334.
19. F. Benabid, G. Bouwmans, J. C. Knight, P. St. J. Russell, and F. Couny, "Ultrahigh Efficiency Laser Wavelength Conversion in a Gas-Filled Hollow Core Photonic Crystal Fiber by Pure Stimulated Rotational Raman Scattering in Molecular Hydrogen," Phys. Rev. Lett. **93**(12), 123903 (2004).
20. F. Couny, O. Carraz, and F. Benabid, "Control of transient regime of stimulated Raman scattering using hollow-core PCF," J. Opt. Soc. Am. B **26**(6), 1209–1215 (2009).
21. E. A. J. Marcatili and R. A. Schmeltzer, "Hollow Metallic and Dielectric Waveguides for Long Distance Optical Transmission and Lasers," Bell Syst. Tech. J. **43**, 431783 (1964).

1. Introduction

Higher-order modes (HOMs) in optical fiber-based systems have enabled numerous new applications in photonics due to their remarkable properties, which may feature a complex transverse spatial intensity pattern, an unconventional polarization texture, a distinctive optical dispersion and a large effective area [1–6]. Different methods have been used for generating HOMs [7–13]. For example, long period gratings in an Er-doped fiber amplifier have been used to convert from the fundamental mode to a circular-symmetric HOM, which was then amplified up to pulse energies of 0.5 mJ at a repetition rate of 10 kHz [14, 15]. A non-invasive, spectrally broad-band, technique for exciting pure HOMs in hollow-core kagomé-style photonic crystal fiber (kagomé-PCF) was recently reported. It is based on prism-assisted side-coupling, and makes use of the fact that the core-guided modes in kagomé-PCF are leaky, i.e., they radiate light sideways from the core. More than twenty different HOMs were individually excited in this way by adjusting the angle of the incident beam, although the injection efficiency was quite low [16]. Here we propose and demonstrate a scheme for amplifying these weak HOMs to high pulse energies, by filling the fiber with hydrogen and using Raman amplification. Raman gain was recently used to amplify HOMs that were synthesized using a spatial light modulator and then end-fire launched into the gas-filled core [17]. Amplification up to pulse energies of 8 μJ were demonstrated for the LP_{01}, LP_{11} and LP_{21} modes. This approach was however limited to relatively low order modes owing to the difficulty of synthesizing complex higher-order modes that precisely match the eigenmodes of the complex and often slightly distorted core structure.

We show in this paper that Raman amplification of side-seeded HOMs can yield pulses with μJ energies carried in a perfect eigenmode of the core. The technique is general and can potentially be applied to the amplification of HOMs of arbitrary order, provided they are guided in the core. We focus our study on six modes: LP_{21}, LP_{02}, LP_{41}, LP_{22}, LP_{03} and LP_{61}, and demonstrate gains exceeding 60 dB and maximum pulse energies of 8 μJ, amounting to more than 20% of the launched pump pulse energy.

The experimental configuration is sketched in Fig. 1(a). The optical source is a Nd:YAG microchip laser delivering 2 ns pulses at a central wavelength of 1064 nm and a repetition rate of 1 kHz. The laser output is split into two paths. In the first, noise-seeded SRS inside a H_2-filled hollow-core photonic bandgap PCF generates a seed pulse at 1135 nm, which corresponds to the first rotational Stokes line of H_2 (Raman frequency shift 17.61 THz [18]). The limited guidance bandwidth of the photonic bandgap PCF allows efficient generation of the first rotational Stokes line since all other Raman processes, including generation of vibrational Stokes and anti-Stokes, are suppressed because of much higher propagation losses

[19]. The Stokes seed pulse is then launched into a single mode fiber (SMF), the output end of which is mounted on a motorized rotation stage. This allows the coupling angle ϕ entering the prism to be chosen so as to selectively excite a single HOM in the kagomé-PCF [16]. Briefly, a collimated beam (1 mm diameter) is focused by a cylindrical lens (focal length of 5 cm) onto the side of the kagomé-PCF, 10 cm distant from its input end (limited by the size of the gas cell). A silica glass prism (1° tilt angle) is used to set the coupling angles to 10° < ϕ < 12°.

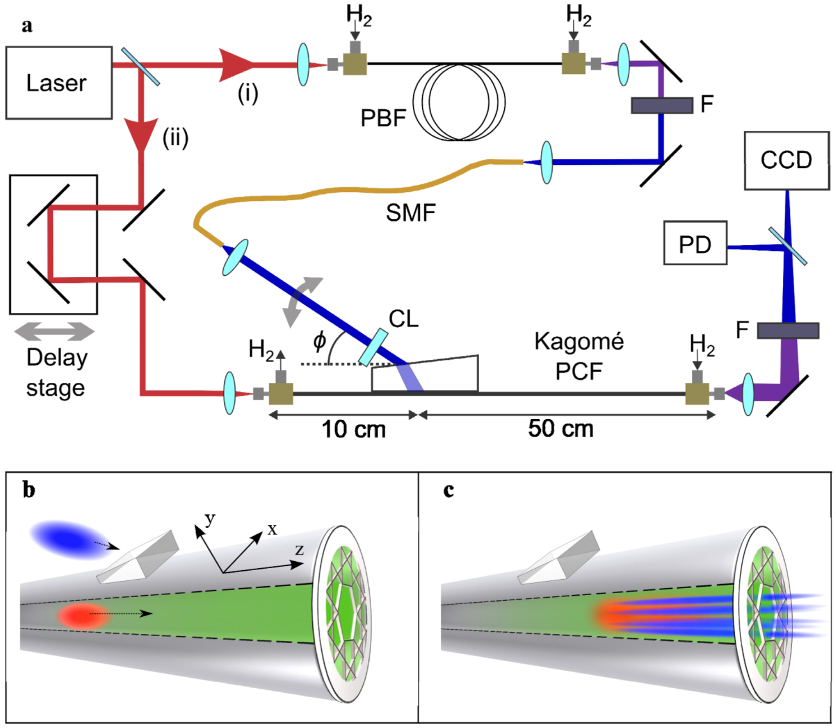

Fig. 1. (a) Experimental configuration for amplifying side-seeded HOMs. Pulses from a Nd:YAG laser (1064 nm) are split into two paths. In path (i), 16 µJ of pump pulse energy is launched into a H_2-filled hollow-core photonic bandgap fiber (PBF), resulting in generation of a pulse at the first rotational Stokes frequency. The remaining pump energy is spectrally filtered out using a dielectric bandpass filter (F) and the Stokes pulse launched into a single mode fiber (SMF) that is mounted on the rotation stage of a side-coupling scheme. By choosing an appropriate coupling angle ϕ, the collimated Stokes light emerging from the SMF is used to seed a pure HOM in a H_2-filled kagomé-PCF (core diameter 37 µm). The pump pulse in path (ii) is injected into the fundamental mode of the kagomé-PCF core. A variable delay line is used to ensure temporal overlap between the co-propagating pump and HOM seed pulses. Over a fiber length of 50 cm, intermodal stimulated Raman scattering (SRS) amplifies the HOM. The spatial profile and pulse energy of the amplified HOM at the output are monitored with a CCD camera and an InGaAs photodiode (PD). (b) Schematic (not to scale) of the system just before the pulses overlap in the kagomé-PCF core. The seed pulse at 1135 nm (blue) is incident on a silica prism (1° tilt angle) placed in contact with the side of the kagomé-PCF. (c) Schematic (not to scale) of the system when the pulses overlap in the core and energy is transferred from the pump to the HOM. The gas pressure gradient from 0 to 4.5 bar (along +z) is represented by green shading.

Although the incident seed pulse energy is 0.4 µJ, less than 0.1 nJ is coupled into the HOM, due to the intrinsically low efficiency of the side-coupling scheme. The second part of the pump pulse, carrying up to 35 µJ energy, is launched into the fundamental mode of the kagomé-PCF. An adjustable delay line allows the temporal overlap between the HOM seed and the pump pulse to be optimized for maximum amplification of the HOM. The remaining pump energy is blocked with a dielectric bandpass filter, and the transverse mode pattern and

#227065 - $15.00 USD Received 18 Nov 2014; accepted 23 Dec 2014; published 14 Jan 2015

pulse energy of the amplified HOM Stokes pulse are measured using a CCD camera and a photodiode.

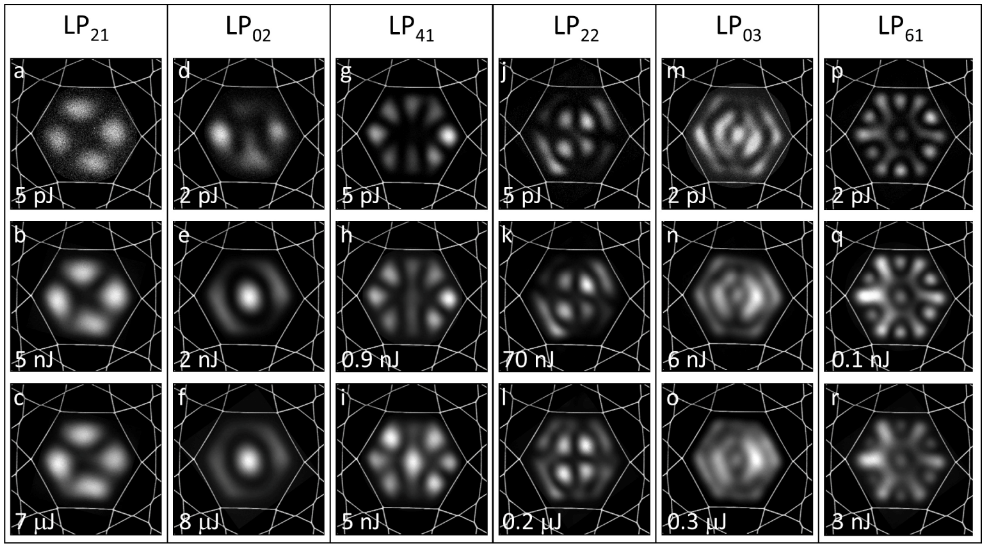

Fig. 2. Normalized spatial intensity profiles of six amplified HOMs measured using a CCD camera. An SEM of the kagomé core structure is superimposed for reference. The upper row shows unamplified or weakly amplified mode profiles with Stokes pulse energies W_S ~2 pJ. On the bottom row, the modes are strongly amplified while preserving their distinctive spatial profile. An intermediate state is displayed in the middle row. The mode order and gains are as follows: (a,b,c) LP_{21}: 0 dB, 30 dB, 61.5 dB; (d,e,f) LP_{02}: 0 dB, 30 dB, 66 dB; (g,h,i) LP_{41}: 9.5 dB, 33 dB, 39.5 dB; (j,k,l) LP_{22}: 20 dB, 61.5 dB, 66 dB; (m,n,o) LP_{03}: 13 dB, 47.8 dB, 64.8 dB; (p,q,r) LP_{61}: 10 dB, 27 dB, 31.8 dB. In addition, the LP_{01}, LP_{11}, LP_{31} and LP_{12} modes were also observed and successfully amplified.

Experimental parameters, such as the length over which the pump and seed pulses overlap, the H_2-gas pressure and the pump pulse energy, can be adjusted to optimize the Raman gain. For constant pressure along the fiber, however, parasitic emission of an unwanted noise-seeded Stokes signal in the fundamental mode decreased the pump pulse energy and distorted the spatial profile of the amplified HOM signal. This could be avoided by establishing a H_2-gas pressure gradient along the fiber, i.e., keeping a constant pressure of 4.5 bar at the fiber output while evacuating the input end. In this way, the nonlinear interaction between pump and HOM seed could be effectively optimized. Over the first 10 cm of fiber, before the Stokes seed is coupled into the fiber, the lower gas pressure reduces the Raman gain and suppresses noise-seeding of the Stokes signal in the fundamental mode. Over the remaining length of fiber, where the HOM seed overlaps with the pump pulse, the Raman gain remains more or less constant for pressures higher than 3 bar [20]. This resulted in the experiment in an amplification length of 50 cm, which while long enough to allow efficient amplification of the HOM, is however short enough to allow detection of unamplified seed pulses. This in turn meant that the Raman gain could be accurately estimated simply by dividing the amplified Stokes power by the unamplified seed power at the fiber output.

We now study the properties of the LP_{21}, LP_{02}, LP_{41}, LP_{22}, LP_{03} and LP_{61} modes for increasing pump pulse energy. A CCD camera was used to monitor the transverse intensity patterns of the excited HOMs, which are linearly-polarized (LP) and can be approximately modeled by analytic solutions for the modes of a dielectric capillary waveguide [21]. Figure 2 shows the spatial patterns of six selected LP modes at different pump pulse energies. Each column corresponds to a different HOM (from left to right: $LP_{21,}$ LP_{02}, LP_{41}, LP_{22}, LP_{03}, and LP_{61} modes, where the first subscript refers to the azimuthal order and the second to the radial

#227065 - $15.00 USD Received 18 Nov 2014; accepted 23 Dec 2014; published 14 Jan 2015

order) in the order of their appearance as ϕ is increased (see Table 1). The three rows compare the measured modal patterns at low, intermediate and maximum Raman gain. When the Raman amplification was switched off, the Stokes seed pulses (with energies as low as 2 pJ) were monitored with a lock-in amplifier. Because of high fiber loss and a low injection efficiency (between 10^{-3} and 10^{-5}), a small amount of gain was needed for the LP_{41}, LP_{22}, LP_{03}, and LP_{61} modes to be detectable by the CCD camera. The losses γ_{dB} of the first four HOMs could be measured using the standard multiple cut-back technique and the results are displayed in Table 1. In the experiments the LP_{01}, LP_{11}, LP_{31}, LP_{12} modes, as well as many others, could also be observed and Raman amplified.

The effect of the different modal losses can be observed in Fig. 2d, where the LP_{02} mode strongly interferes with the LP_{21} mode. Although the angle ϕ is selected to maximize excitation of the LP_{02} mode in the fiber, the neighboring LP_{21} mode ($\phi_{02} - \phi_{21} = 0.06°$) is also weakly excited due to the unavoidable angular spread of the side-coupled beam. After a 50 cm propagation length, the attenuation of the LP_{02} mode is 200 times higher than the LP_{21} mode (calculated from γ_{dB}). As a result we observe, at the fiber output, a mixture of the two modes even if the LP_{21} mode intensity is negligible compared to the LP_{02} intensity at the side-coupling position. The high quality of the LP_{02} mode spatial profile is however retrieved when the amplification is switched on. For all modes shown in Fig. 2, an amplification factor of ~30 dB can be obtained while preserving a highly pure mode profile. Increasing the pump energy W_P up to 35 μJ produces gains greater than 60 dB, allowing HOMs to be generated with energies in the μJ range. The transverse profiles of LP_{21}, LP_{02}, LP_{22} and LP_{03} modes are conserved under maximum Raman amplification, Stokes pulse energies W_S = 7 μJ, 8 μJ, 0.2 μJ and 0.3 μJ being respectively reached. The LP_{61} mode also remains distinctive during amplification. However, amplification of this mode is accompanied by noise-seeded SRS in the fundamental mode that blurs the modal profile when W_P increases above 25 μJ (Fig. 2r). For the LP_{41} mode, another competing Raman process prevents us from reaching gain values greater than 40 dB without affecting its characteristic spatial profile. Here again, a weakly coupled neighboring mode (LP_{02} with $\phi_{41} - \phi_{02} = 0.41°$) comes into play. For $W_P > 20$ μJ, we observe, along with amplification of the LP_{41} mode, the buildup of a Stokes pulse with the transverse intensity profile of the LP_{02} mode. Each HOM triggers its own stimulated Raman emission and, even though the injected LP_{02} energy is very low, dual modal amplification occurs because of the larger spatial overlap F between the LP_{02} seed pulse and the LP_{01} pump pulse (see discussion below and Table 1).

Table 1. Measured optical parameters of HOMs

HOM	LP_{21}	LP_{02}	LP_{41}	LP_{22}	LP_{03}	LP_{61}
ϕ (°)	10.86	10.92	11.33	11.44	11.5	11.6
γ_{dB} (dB/cm)	0.02	0.48	0.34	0.7	–	–
F	0.65	0.86	0.50	0.73	0.77	0.58

Figure 3 shows the Stokes output pulse energy W_S monitored as W_P is increased. The amplification of the injected Stokes can reach more than six orders of magnitude. The highest values of W_S were 7 μJ and 8 μJ, obtained for the two lowest order modes (coupled at the lowest values of ϕ in Table 1) observed in this experiment, namely the LP_{21} and LP_{02} modes. The LP_{41} and LP_{61} modes are monitored up to W_P = 25 μJ, above which their amplified transverse profiles change shape as discussed previously.

For $W_P < 20$ μJ, W_S increases exponentially corresponding to a straight line on the semi-log graph in Fig. 3 with a characteristic slope proportional to the Raman gain. We compare the experimental results with a theoretical intermodal Raman gain model [18]:

$$\frac{\partial W_S}{\partial z} = \left(\frac{gF}{A_P\, t_{eff}} W_P(z) - \alpha_0 \right) W_S, \tag{1}$$

#227065 - $15.00 USD Received 18 Nov 2014; accepted 23 Dec 2014; published 14 Jan 2015

where α_0 is the linear loss of HOM. The total gain is the product of the intrinsic Raman gain g, the pump intensity in the core $W_P(z)/(A_P t_{eff})$ and the intensity overlap integral F between pump and Stokes modes. Expressions for the effective pump area A_P, the effective pulse duration t_{eff} and F are given in [17].

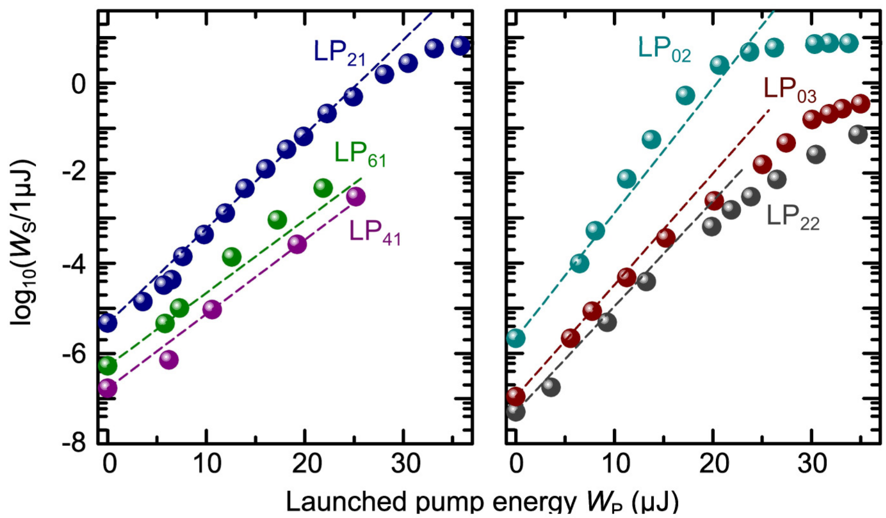

Fig. 3. The measured Stokes output pulse energies (spheres) of six HOMs plotted as a function of launched pump pulse energy. The lines correspond to solutions of Eq. (2) for g = 0.5 cm/GW. For clarity, the experimental results are separated into two graphs with three modes in each.

In the experiment, A_P = 500 μm^2, t_{eff} = 6 ns and the values of F are given in Table 1 (calculated from the recorded transverse spatial profiles of each HOM). A constant Raman gain of g = 0.5 cm/GW is assumed along a length L = 50 cm of the fiber and pump depletion is neglected. The analytical solution of Eq. (1) is then:

$$W_S(z) = W_S(0)\exp\left(\frac{gF}{A_P t_{eff}} W_P - \alpha_0\right) z. \qquad (2)$$

Experimentally it was straightforward to measure the energy in the Stokes pulse at zero Raman gain, i.e., $W_S(0)\exp(-\alpha_0 L)$. Theory could then be compared with experiment by substituting this measured value into Eq. (2) and evaluating the Stokes energy for increasing values of pump energy W_P. The results are plotted in Fig. 3 (dashed lines) along with the experimental data (spheres). For W_P < 20 μJ, there is good agreement – the varying overlap integrals F determine the slopes of the lines for each HOM. Note that the gain of the LP_{02} mode (F = 0.86), is almost twice that of the LP_{41} mode (F = 0.50). This causes the effect observed at W_P > 25 μJ (Fig. 2i), where a weakly coupled LP_{02} Stokes seed pulse can be amplified to energies comparable to an originally much stronger injected LP_{41} Stokes seed pulse.

As seen in Fig. 3, saturation effects begin to appear at W_P > 25 μJ, when the simple model described by Eq. (1) is no longer valid. We investigated this regime experimentally by monitoring the output pump and seed pulse energies $W_P(L)$ and W_S at exit from the fiber. These components were selected with dielectric bandpass filters and are displayed as a function of W_P in Fig. 4. When a LP_{02} seed was injected by side-coupling, it could be amplified up to W_S = 8 μJ, which is a value comparable to the pump energy. Such efficient energy transfer into the HOM Stokes mode depletes the pump significantly, an effect that can be seen by comparing $W_P(L)$ with the extrapolated output pump energy in the absence of

#227065 - $15.00 USD Received 18 Nov 2014; accepted 23 Dec 2014; published 14 Jan 2015

nonlinear effects (full red line). This causes the total Stokes gain to fall, and is responsible for the saturation dynamics of the amplified LP_{02} and LP_{21} modes in Fig. 3. In this regime of high Raman gain, where the Stokes energy quickly reaches a relatively large fraction of the pump energy, we detect less than 0.2 µJ of unwanted noise-seeded Stokes or anti-Stokes. As expected, in Fig. 4 the sum of the pump and Stokes pulse energies $W_P(L) + W_S$ is equal, within experimental error, to the total pulse energy W_{tot} measured experimentally when the entire output signal is collected (i.e., no spectral filters are used). By comparing W_{tot} to the full line in Fig. 4, we can estimate the energy loss in the system, which is mainly caused by the much higher propagation loss of the LP_{02} Stokes mode (0.48 dB/cm) compared to the fundamental mode (0.01 dB/cm).

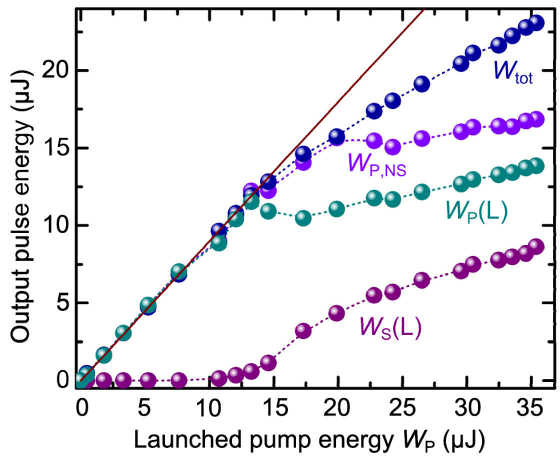

Fig. 4. The pump (1064 nm) and amplified LP_{02} Stokes (1135 nm) pulses are frequency selected with bandpass filters and their output pulse energies $W_P(L)$ and $W_S(L)$ measured as the pump energy is increased. The sum of the pulse energies in all the spectral components W_{tot} is measured at the fiber output by removing the spectral filters. The transmitted pump pulse energy in the absence of any seed, $W_{P,NS}$, saturates at around 20 µJ. The full red line is the theoretical maximum pump output energy, extrapolated from $W_P(L)$ at low energies. In these measurements, the H_2 gas pressure increased from 0 to 7.5 bar along the fiber.

If the seed pulse energy remained negligible compared to the co-propagating pump pulse energy (as is the case for the LP_{41}, LP_{22}, LP_{03} and the LP_{61} modes), we detected for large pump energies a first vibrational Stokes line at 1908 nm (Raman shift 124.65 THz for H_2 [18]), generated by noise-seeded stimulated Raman scattering. To investigate this regime, we monitored the output pump energy in the absence of a Stokes seed, $W_{P,NS}$. Significant pump depletion was once again observed, causing the saturation dynamics of the amplified LP_{22} and LP_{03} modes seen in Fig. 3. Note that the generation of the vibrational Raman Stokes line could be suppressed by increasing the injected seed pulse energy.

In summary, pure single HOMs with high pulse energy can be produced in hydrogen-filled kagomé-PCF using Raman amplification of a side-seeded HOM at the Stokes frequency. The modes can be amplified by more than 60 dB (limited by pump depletion and competing Raman processes) without degradation of the transverse mode profile. The maximum observed HOM pulse energy of 8 µJ could be greatly increased if higher seed and pump energies are used. The synthesis of pure high power HOMs may be important in advanced studies of optical trapping, as well as in molecular and trace-gas sensing based on intermodal stimulated Raman interactions in hollow-core fibers.

Acknowledgments

We would like to thank Tijmen Euser for insightful discussions.